Int j simul model 22 (2023) 1, 88-99
Original scientific paper

SIMULATION ANALYSIS OF TEMPERATURE FIELD OF TINPLATE IN THE QUENCHING

Zhang, W. J.[*]; Zhang, X. D.[*]; Guo, Z. F.[*]; Wang, J. H.[*] & Bai, Z. H.[*,**,#]

[*] National Cold Rolling Strip Equipment and Process Engineering Technology Research Center of Yanshan University, Qinhuangdao, 066004, China

[**] State Key Laboratory of Metastable Materials Science and Technology, Yanshan University, Qinhuangdao, 066004, China

E-Mail: bai_zhenhua@aliyun.com ([#] Corresponding author)

Abstract

To reduce the defect of quench stain on tinplate's surface in the reflow section of the tinplating unit, based on the equipment and process parameters, the quench stain was analysed and the treatment strategy was proposed, which added nozzles to hasten the heat exchange of the strip into the quenching tank. A three-dimensional finite element model was constructed by Creo and ANSYS to reduce the correction rate of quench stain and reveal the temperature field of tinplate in quenching tank. The factors of quenching time, nozzle jet speed, nozzle angle, nozzle pressure, and nozzle size on the tinplate temperature field were analysed. Results show that the temperature field of the tinplate is relatively uniform when the nozzle jet speed of the nozzle is 1m/s, the nozzle angle is 15°, the nozzle pressure is 0.3 MPa, and the nozzle size is 5 mm. The quenching equipment is reformed to verify the result of the simulation. The defect correction rate of quench stain on the strip decreases from 1.79 % to 1.03 % in the tinplating unit, which meets the accuracy of the simulation analysis. The obtained conclusions provide a reference for treating quench stain in the tinplating unit.

(Received in September 2022, accepted in January 2023. This paper was with the authors 3 weeks for 1 revision.)

Key Words: Tinplate, Quench Stain, Temperature Field, Finite Element

1. INTRODUCTION

Tinplate is often used in the food packages; its surface quality is the most important index to measure the corrosion resistance and aesthetics of food packages [1]. The production of tinplate is long and the technology is complicated, which leads to the surface quality being influenced by many reasons. The hot rolling, cold rolling, annealing, and secondary cold rolling mainly affect quality defects such as slag inclusion, oxidation sheet, and emulsion stain on the surface of the tinplate's substrate [2-4]. The electroplating process mainly affects quality defects such as pinholes, black grey and quench stain on the surface of the tinplate [5].

With the transforming and upgrading of the high-end manufacturing industry and expansion of tinplate products, the surface defect control technology of the tinplate's substrate and the electroplating process of tinplate are gradually maturing. The reflow and passivation become the most simple and effective technology to improve the surface quality of the tinplate after electroplating. The surface quality defects of tinplate commonly include pinholes and spots in the reflow section of the tinplating unit. Although the pinhole defects can be cured by the reflow, it will lead to form quench stain on the surface of the tinplate after quenching. At present, there are two main studies on the formation of quench stain on tinplate. Some researchers think that quench stain is caused by impurities attached to the tin layer in the quenching tank [6]. Others believe the quench stain is the quality defect caused by the relative sliding scratch between the surface of the tinplate and the roll [7]. Through field technical analysis, this study think that the tin layer is not evenly distributed on the surface of the tinplate, which results in a visual colour difference, namely the quench stain. Therefore, varying of the temperature field of the tinplate is the main reason affecting the formation of quench stain. During the quenching, the variation of the temperature field on the tinplate is

affected by the speed of the tinplating unit, nozzle jet speed, nozzle angle, nozzle pressure, nozzle size, quenching temperature, and other factors. With the improvement of finite element method (FEM), applying Fluent for transient and steady-state analysis of temperature field becomes more convenient [8]. Dorfman [9] studied the transient heat transfer between thin plate and thin liquid film and calculated the temperature of the moving front of the plate, the film speed and the time needed to reach the wetting temperature. Zhang et al. [10] analysed the temperature difference between the middle and the edge of a thick strip quenching. Wang et al. [11] adopted the method of computational fluid to analyse the influence of the inlet and outlet size of the cold plate, coolant flow rate, and inlet and outlet location on the maximum temperature and temperature difference of plate under steady-state condition.

Many researchers have conducted basic studies on the temperature field distribution under the different cooling conditions of thin plates. But there are a little theoretical analysis and applications for the thin plates under the coupling condition of multiple physical fields. Therefore, it has become the urgent problem to study the influence of nozzle structure parameters of the quenching tank on the temperature field of tinplate to improve the surface quality of tinplate. The purpose of the study is to analyse the formation of the quench stain on the tinplate and the influence of the nozzle on the quench stain on the tinplate. According to the results of the simulation analysis, the structure of the quenching tank was optimized to reduce the quench stain on the surface of the tinplate.

2. STATE OF THE ART

There is little direct research on the temperature field of tinplate during the quenching. The research on the strips mainly focuses on the analysis of the flow field in quenching, the structure of the quenching tank, and the change of the microstructure and mechanical properties of the strip during the quenching.

Some scholars have studied the flow field distribution and optimization of the quenching tank. Chen et al. [12, 13] used computational fluid to simulate the flow speed distribution in the quenching tank, which improved the uniform distribution of flow in the quenching tank. Yang et al. [14] used Fluent software to simulate the flow distribution of the quenching tank, and they studied the influence on the flow rate with a stirring system. Fu et al. [15] analysed the internal between the cooling rate and microstructure of nickel-base superalloy by simulation and verified the relationship between cooling rate and metallography by experimental means. Qu et al. [16] designed a physical model of intense quench equipment with a double vortex and used Fluent software to analyse the flow field of the optimized quenching tank, which improved the strength of the workpiece in quenching. Zhang et al. [17] simulated the temperature field change of the steel quench and cooling in the roller quench machine, and they completed developing the control of quench machine based on this model. Zhang et al. [18] simulated the layout of the guide tube of the large aluminium ring quenching tank to scatter the medium flow field in the cooling zone and the flow speed curve at the inner and outer sides. According to the simulation results, they optimized the layout of the guide tube and the guide flow equalization. Wang et al. [19] used the fluid-structure coupling numerical simulation method to simulate the flow field of the quench oil tank and optimize the circulation of quenched oil tank in the combined well unit under the results of simulation.

Many scholars have carried out finite element simulation on the mechanical properties of medium and thick plates during quenching. Cebo-Rudnicka and Malinowski [20] studied the effects of water flux rate, fluid pressure, and distance from the nozzle to the plate on the boiling curve features of plate surface by using FEM solvers with linear and nonlinear shape works. Li et al. [21] used ANSYS implicit finite element method to simulate the controlled cooling of a 50 mm thick plate, and they analysed the influence of different cooling methods

on the temperature uniformity of the section. Liu et al. [22] showed a numerical simulation model for the surface temperature rise of steel plate after laminar cooling, the hastened cooling and improved the mechanical properties of thick plate. Arora et al. [23] simulated the temperature field distribution and transverse deformation of the weld centre of low-carbon steel. Lee et al. [24] analysed the influence of moving speed and location of heat source on the temperature distribution and permanent deformation of SS400 carbon steel by FEM.

The previous studies mainly use FEM to analyse the speed distribution of the flow field in the quenching tank and the mechanical properties of the thick plate during the cooling. However, there are few studies on the influence of the cooling on the surface defects of the workpiece, especially the influence of the quenching tank on the temperature field distribution of the workpiece and optimization. Based on the research on the formation mechanism and treatment measures of quench stain on the surface of tinplate, this study simplified the structural model of quenching tank, analysed the influence of nozzle structural parameters on the temperature field of tinplate using FEM, and compared the correction rate of quench stain on tinplate before and after the optimization of quenching tank through the technical application.

3. METHODOLOGY

3.1 Mechanism of quench stain in tinplate

The process of tinplate is shown in Fig. 1. To reduce the problems of needle holes and improve the adhesion, compactness, and uniformity of the tin layer on the strip surface, the surface temperature of the strip is heated above the tin melting point through combined reflowing. To avoid the oxidizing the tin layer on the surface of the tinplate after reflowing and forming the bright tin layer at the same time, it is generally quenching progress. However, the quench stain will be formed on the tinplate surface.

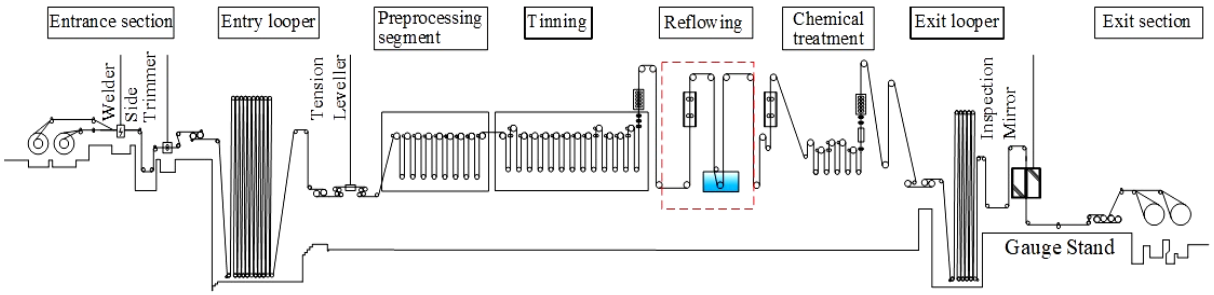

Figure 1: Flow chart of the tinplating unit.

After reflowing, the surface temperature of the tinplate reaches 538 K, and the temperature of the quenching tank is kept between 353 K and 363 K under the control of 373 K steam and 293 K freshwater. At this time, the temperature difference reaches 175 K-185 K between the tin layer on the strip surface and the water in the quenching tank. As shown in Fig. 2, the tinplate is in the transitional boiling zone. According to the boiling heat transfer theory [25], the generation of bubbles on the strip surface is unstable. The bubbles adhere to the strip surface, which leads to the difficulty of steam carry out, the decrease of heat flux, and the slow heat transfer. At the same time, the bubble is easy to burst and will have an impact force on the molten tin layer on the strip surface, resulting in the uneven tin layer and quench stain.

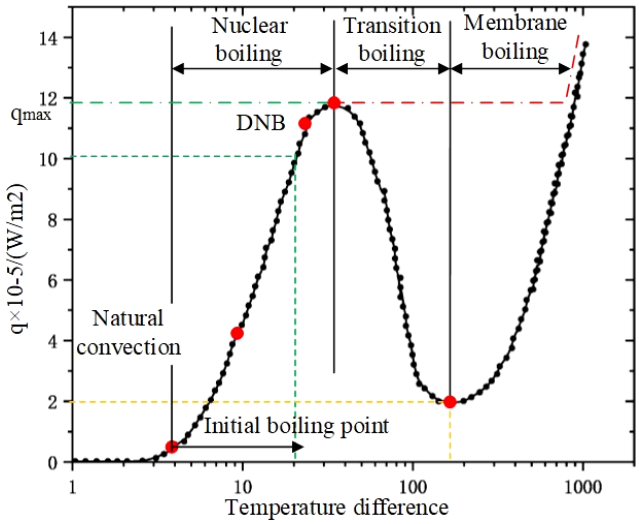

Figure 2: Between boiling heat transfer coefficient and temperature difference.

As shown in Fig. 3, the nozzles are added in the quenching tank and increased the flow field of tinplate entering the quenching tank. On the one hand, which breaks the steam film on the tinplate surface, improves the heat flux, and hastens the tinplate cooling. On the other hand, the bubbles are taken away to reduce the impact on the tin layer on the tinplate surface, which reduces the chance of quench stain.

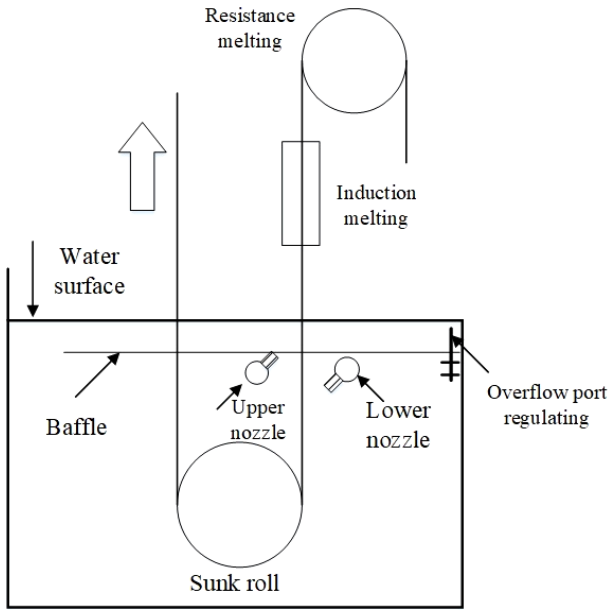

Figure 3: Diagram of the quenching tank.

The nozzle jet speed, nozzle angle, nozzle pressure and nozzle size are all set according to the experience. Therefore, to reduce the quench stain on the tinplate surface, some reasons need to be simulated to provide a reference for the nozzle in the quenching tank.

3.2 Geometric modelling

The quenching tank is shown in Fig. 4 and the parameters of the quenching tank are listed in Table I. To simplify the study of the temperature field of the tinplate, the following assumptions are made for the flow field of the quenching tank: (1) Ignoring the interference of the sunk roll. (2) The flow state of water in the quenching tank is steady. (3) Ignoring the

influence of air on the water surface of the quenching tank. The Creo was used to establish the structure model of the quenching tank, which is imported into Workbench2020. Subsequently, the inlet, outlet, and fluid-structure coupling boundary of the quenching tank are named. The finite element model of quenching under the static state was established to simulate the quenching.

Table I: The geometry model's parameters of the quenching tank.

Parameters	Values
Length × width × height of quenching tank (mm)	300 × 190 × 350
Length × width × height of tinplate (mm)	260 × 1.5 × 300
Distance from the lower nozzle to the water surface (mm)	135
Distance from the upper nozzle to the water surface (mm)	110
Distance from the outlet to the bottom of tank (mm)	100
The diameter of the outlet (mm)	∅15
The thickness of tinplate (mm)	1.5

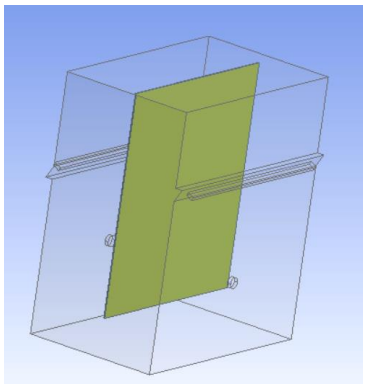

Figure 4: Geometric model of quenching tank.

3.3 Meshing

The flow field characteristics of the quenching tank should be considered in meshing [26, 27]. Since the quenching tank and the tinplate are relatively regular, the tetrahedral mesh is used for meshing. The solver is set as Fluent, the size is set as 4 mm, and the smoothness is set as high. The meshing result of the quenching tank is shown in Fig. 5 a and the meshing result of the tinplate is shown in Fig. 5 b.

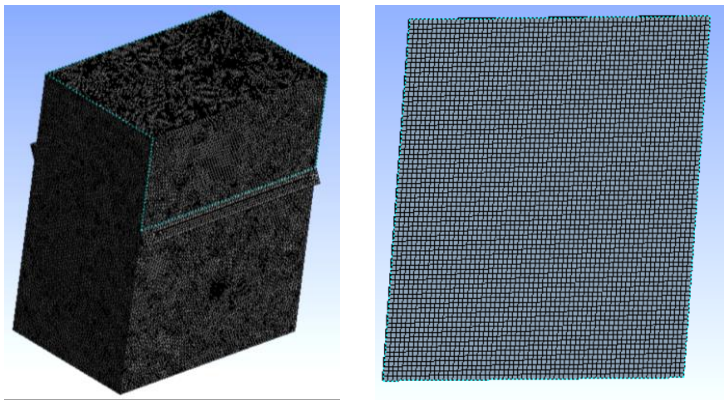

a) b)

Figure 5: Meshing of the quenching tank and tinplate; a) meshing of the quenching tank, b) meshing of tinplate.

3.4 Boundary conditions and parameters setting

Importing the geometric model of the quenching tank and tinplate into Fluent, and the boundary conditions of the continuous phase model were set, as shown in Table II.

Table II: Setting of the boundary conditions of the quenching tank.

Boundary condition	Parameters setting
Solver	Pressure solver
Energy equation	Open
Turbulence Models	$k-\varepsilon$
Turbulence intensity (%)	8
The temperature of the water in the tank (K)	353
The temperature of the water injected (K)	293
The temperature of the Tinplate (K)	538
Convective heat transfer coefficient (W/(m^{2}·K))	50
Nozzle inlet	Velocity-inlet

4. RESULT ANALYSIS AND DISCUSSION

4.1 Effect of cooling time on temperature field of tinplate

The angle of the upper and lower nozzles is set as ±15° respectively, and the temperature field distribution on the surface of the tinplate is obtained when cooling 0.5 s, 1 s, 1.5 s and 2 s. The result is shown in Fig. 6 and the tinplate begins to cool from 538 K. With the increasement of cooling time, the overall temperature of the tinplate decreases to 348 K-376 K, and the temperature of the tinplate surface around the nozzle decreases to 348 K-362 K. However, the temperature of the tinplate edge decreases to 418 K-432 K. Besides, it can be seen that a faster temperature drops in the central area and a slower temperature drops at the edge of the tinplate, which is caused by cooling nozzle. The simulation results can be used for optimizing speed in the tinplating unit.

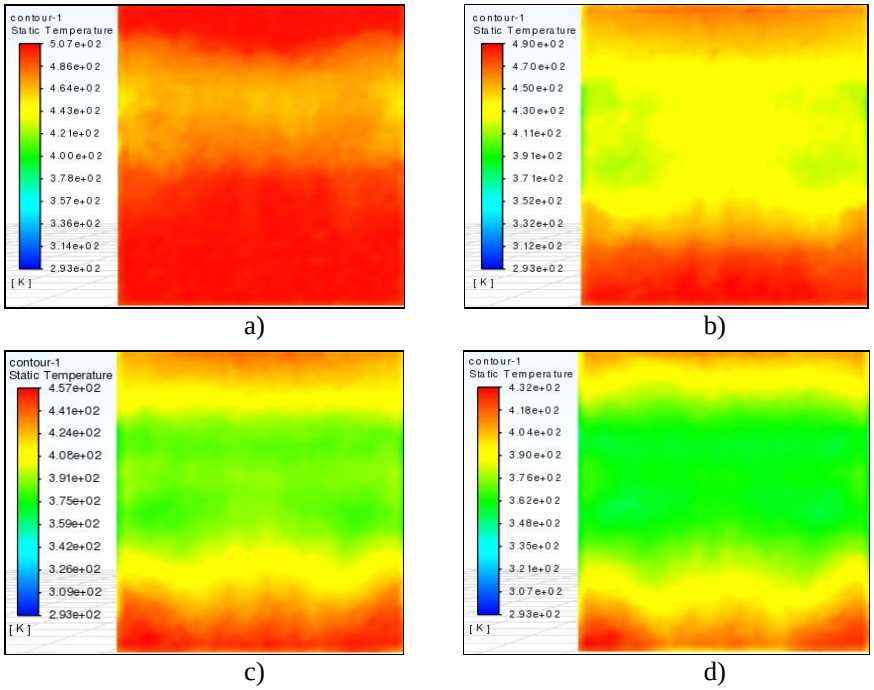

Figure 6: Temperature field of tinplate with different cooling times; a) 0.5 s, b) 1 s, c) 1.5 s, d) 2 s.

4.2 Effect of nozzle angle on temperature field distribution of tinplate

The angle of the upper and lower nozzles is set as 0°, ±15°, ±30° and ±45° respectively, and other boundaries settings are listed in Table III. The influence of different nozzle angles on the temperature field of the tinplate is analysed and the simulation results are shown in Fig. 7. According to the simulation results, when the nozzle angle gradually increases, the temperature field on the surface of the tinplate gradually changes from one bright ripple band to two ripples. When the nozzle angle is between 0° and 15°, the overlapping two ripples gradually separate, the overall temperature drop becomes faster and the uniformity of the temperature field becomes better. When the nozzle angle is between 15° and 30°, the nozzle angle becomes larger, the temperature field ripple gap becomes larger and its uniformity becomes worse. When the nozzle angle exceeds 30°, the upper nozzle jet exceeds the range of the quenching tank, and only the lower nozzle is used for cooling. To sum up, it is more suitable to set the nozzle angle to 15°.

Table III: Settings of influences of the nozzle angle on plate temperature field.

Parameters	Values
Nozzle inlet jet speed (m/s)	1
Water temperature of the quenching tank (K)	353
Tinplate temperature (K)	538
Freshwater temperature (K)	293
Nozzle width (mm)	5

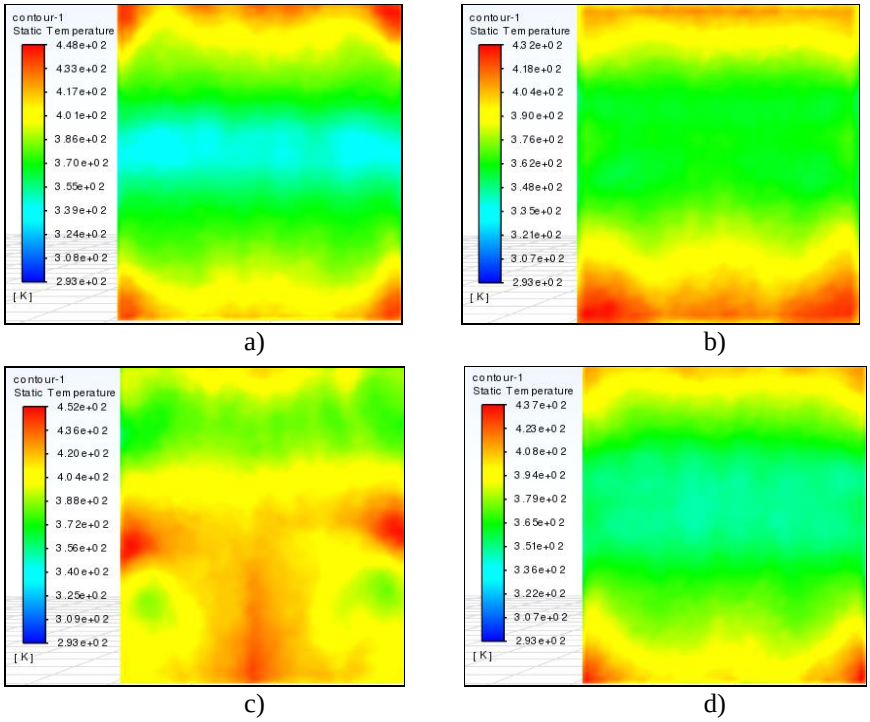

Figure 7: Temperature field of the tinplate at different nozzle angles; a) 0°, b) 15°, c) 30°, d) 45°.

4.3 Effect of inlet jet speed on temperature field distribution of tinplate

The jet speed of the nozzle is set as 0.5 m/s, 0.75 m/s, 1 m/s, 1.25 m/s, 1.5 m/s and 1.75 m/s, respectively. The other boundaries settings are listed in Table IV. The influence of different nozzle jet speed on the temperature field of the tinplate is analysed and the simulation results are shown in Fig. 8. According to the simulation results, the higher the jet speed of the nozzle,

the better temperature uniformity on the surface of the tinplate. The greater the flow velocity of the nozzle, the more intense the movement of the cooling water, and the higher the turbulence degree of the flow field of the quenching tank. So, the cooling water forms an effective quenching zone at the inlet of tinplate in the quenching tank. In the production, the faster the jet speed means the higher water consumption, so the best nozzle jet speed is 1 m/s.

Table IV: Setting for analysing influence of the jet speed on temperature field.

Parameters	Values
Nozzle angle (°)	0
Water temperature of quenching tank (K)	353
Tinplate temperature (K)	538
Freshwater temperature (K)	293
Nozzle width (mm)	5

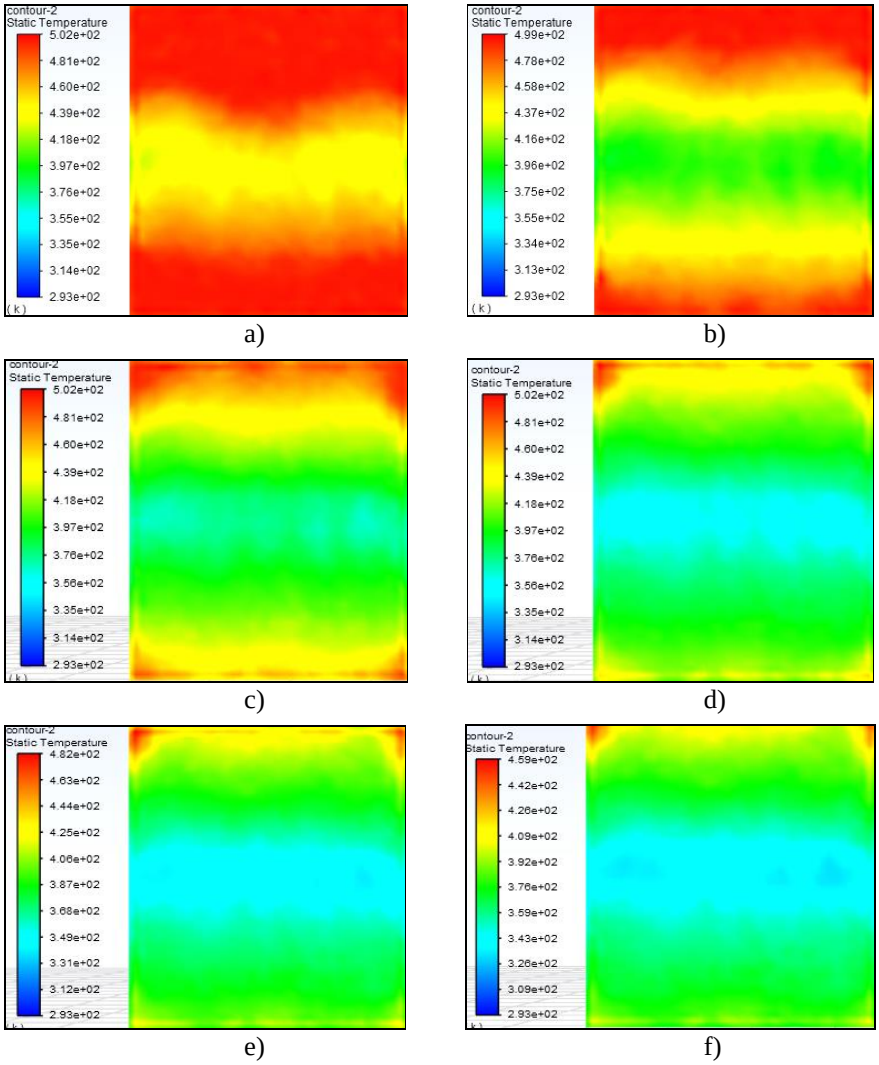

Figure 8: Temperature field of tinplate with different nozzle jet speed; a) 0.5 m/s, b) 0.75 m/s, c) 1 m/s, d) 1.25 m/s, e) 1.5 m/s, f) 1.75 m/s.

4.4 Effect of nozzle pressure on temperature field distribution of tinplate

The nozzle inlet pressure is set as 0.2 MPa, 0.3 MPa, 0.4 MPa and 0.5 MPa, respectively. The other boundaries settings are listed in Table V. The influence of nozzle inlet pressure on the

temperature field of the tinplate is analysed and the simulation results are shown in Fig. 9. According to the simulation results, the greater the nozzle pressure, the faster the cooling rate of the tinplate temperature field, but the temperature uniformity on the surface of the tinplate is also getting worse. The influence of nozzle pressure and nozzle jet speed on the temperature field is same. In the production, higher pressure means higher energy consumption, so the best nozzle pressure is 0.3 MPa.

Table V: Setting for analysing influence of nozzle pressure on temperature field.

Parameters	Values
Nozzle angle (°)	0
Water temperature of the quenching tank (K)	353
Tinplate temperature (K)	538
Freshwater temperature (K)	293
Nozzle width (mm)	5

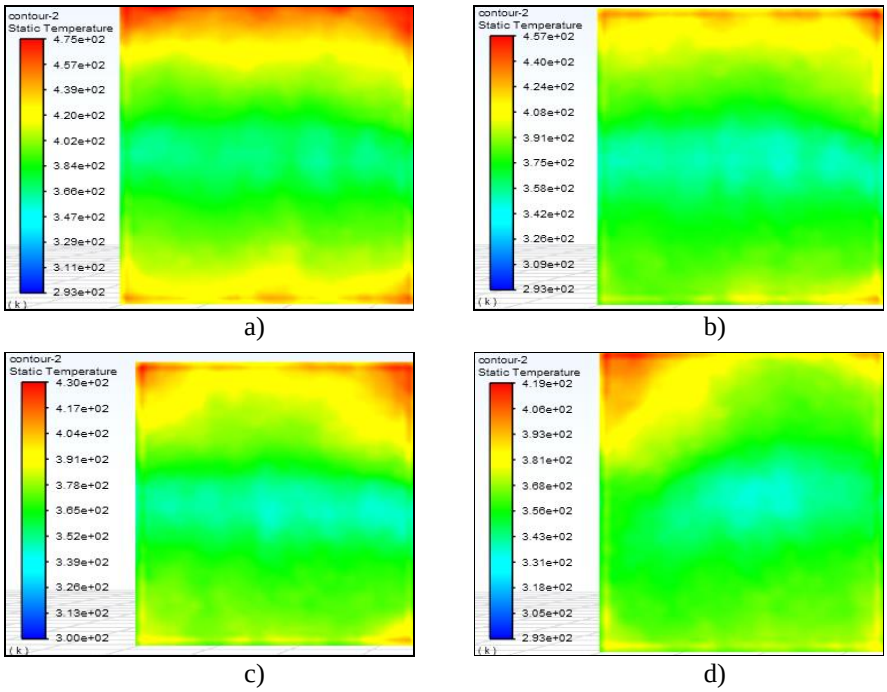

Figure 9: Temperature field of the tinplate with different nozzles pressure; a) 0.2 MPa, b) 0.3 MPa, c) 0.4 MPa, d) 0.5 MPa.

4.5 Effect of nozzle size on temperature field distribution of tinplate

The nozzle widths are set as 2 mm, 3 mm, 4 mm and 5 mm, respectively. The other boundaries settings are shown in Table VI.

Table VI: Settings for analysing influence of nozzle size on plate temperature field.

Parameters	Values
Nozzle inlet jet speed (m/s)	1
Nozzle angle (°)	0
Water temperature of quenching tank (K)	353
Tinplate temperature (K)	538
Freshwater temperature (K)	293

The influence of nozzle widths on the temperature field of the tinplate is analysed and the simulation results are shown in Fig. 10. According to the simulation results, the inlet speed decreases as the width of the nozzle increases. However, due to the close distance between the nozzle and the tinplate, the speed of the cooling water reaching the surface of the tinplate is almost the same. Besides, the larger width of the nozzle means a larger contact area between the cooling water and the tinplate. Therefore, the best nozzle width is 5 mm.

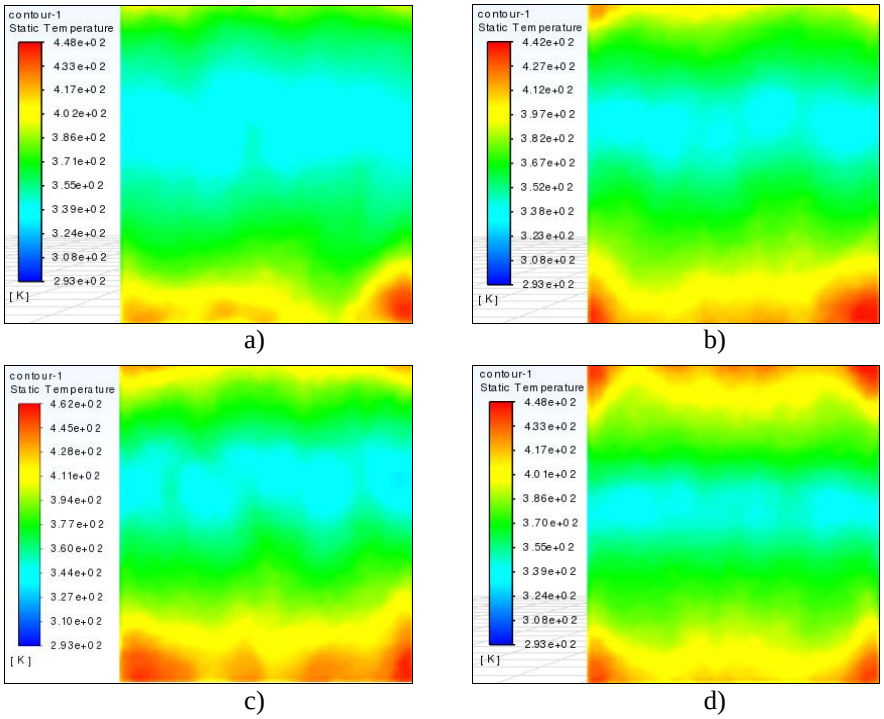

Figure 10: Temperature field distribution of tinplate with different nozzle sizes; a) 2 mm, b) 3 mm, c) 4 mm, d) 5 mm.

5. CONCLUSION

Based on the preliminary analysis of the formation and treatment measures of the quench stain on the tinplate, the finite element model of the quenching was established to find out the influence of nozzle structural parameters on the uniformity of the temperature field of tinplate during the quenching by FEM. Through theoretical research and experimental confirmation, the following conclusions were obtained:

(1) The essence of the quench stain defect is the colour difference caused by the uneven thickness difference of the tin layer on the surface of the tinplate. It is mainly caused by the impact of bubble rupture on the surface of the tinplate when the strip enters the quenching tank. By adding nozzles in the quenching tank, the heat transfer can be accelerated, the time of transition boiling stage can be reduced, and the chance of quench stain can be reduced.

(2) When the nozzle jet speed of the quenching water tank nozzle is 1 m/s, the nozzle angle is 15°, the nozzle pressure is 0.3 MPa, and the nozzle width is 5 mm, the temperature field of the tinplate in the quenching tank is relatively uniform.

(3) The simulation results of the nozzle in the quenching tank have been applied to a tinplating unit and the correction rate of the quench stain decreases from 1.97 % to 1.03 % within one week before and after optimizing of the nozzle.

The research provides a basic reference for treating quench stain in the tinplating unit. However, there are many reasons affecting the strip temperature field during quenching. Therefore, to further improve the simulation results of tinplate surface temperature, the

following reasons should be considered such as tinplate speed, sunk roll flow field disturbance and heat source.

ACKNOWLEDGEMENT

This work was supported by the Special Funding Project Transformation of Major Scientific and Technological Achievements in Hebei Province (22281001Z), and the Science and Technology Project of Hebei Education Department (CXY2023012), China.

REFERENCES

[1] Yildirim, K.; Kizilkaya, A. C. (2022). Effect of the combination of organic acid solutions on tinplate corrosion, *Materials Chemistry and Physics*, Vol. 291, Paper 126742, 10 pages, doi:10.1016/J.MATCHEMPHYS.2022.126742

[2] Li, X. A.; Wang, N.; Chen, M.; Ma, T. Y. (2021). Tracking large-size inclusions in al deoxidated tinplate steel in industrial practice, *ISIJ International*, Vol. 61, No. 7, 2074-2082, doi:10.2355/ISIJINTERNATIONAL.ISIJINT-2020-679

[3] Wilson, P. R.; Chen, Z.; Killmore, C. R.; Liard, S. J.; Williams, J. G. (2007). Surface oxidation of low carbon steel strip during batch annealing, *ISIJ International*, Vol. 47, No. 1, 114-121, doi:10.2355/isijinternational.47.114

[4] Newland, J.; Arnold, J. C. (2009). Influence of production parameters on surface energy of tinplate, *Ironmaking & Steelmaking: Processes, Products and Applications*, Vol. 36, No. 6, 456-461, doi:10.1179/174328109X422557

[5] Huang, X.-Q.; Lang, F.-J.; Ma, Y.; Chen, Y.; Zhang, Z.; Zhang, J.-Q. (2014). Effects of reflowing temperature and time on alloy layer of tinplate and its electrochemical behavior in 3.5% NaCl solution, *Transactions of Nonferrous Metals Society of China*, Vol. 24, No. 6, 1978-1988, doi:10.1016/S1003-6326(14)63279-9

[6] Chakraborty, S.; Giri, S. S.; Bhagat, A. N.; Singh, S.; Ghori, J. (2022). Effect of tramp oil ingress in cold rolling oil bath leading to white spot defect on CRCA at tinplate mill, *Engineering Failure Analysis*, Vol. 140, Paper 106601, 9 pages, doi:10.1016/J.ENGFAILANAL.2022.106601

[7] Wang, J.; Du, M. S.; Wang, F.; Fang, J. C. (2013). Cause analysis on "white spot" surface defect of tinplate, *Steel Rolling*, Vol. 30, No. 4, 16-18, doi:10.13228/j.boyuan.issn1003-9996.2013.04.013

[8] Bhanot, V.; Dhumane, R.; Petagna, P.; Cioncolini, A.; Iacovides, H.; Ling, J.; Aute, V. (2019). Development of a numerical tool for dynamic simulations of two-phase cooling systems, *International Journal of Simulation Modelling*, Vol. 18, No. 2, 302-313, doi:10.2507/IJSIMM18(2)476

[9] Dorfman, A. (2004). Transient heat transfer between a semi-infinite hot plate and a flowing cooling liquid film, *ASME Journal of Heat and Mass Transfer*, Vol. 126, No. 2, 149-154, doi:10.1115/1.1650389

[10] Zhang, Y.; Xu, G.; Yu, Y.; Yang, H. L.; Zhou, M. X. (2014). The simulation of temperature field of 12Cr2Mo1R ultra thick plate for pressure vessels during heat treatment by 3D-FEM, *Applied Mechanics and Materials*, Vol. 556-562, 472-475, doi:10.4028/www.scientific.net/AMM.556-562.472

[11] Wang, T.; Zhang, X.; Zeng, Q. L.; Jiang, S. B.; Zhang, Y. N. (2022). Modelling and simulation on cavity cold plate for Li-ion battery thermal management, *International Journal of Simulation Modelling*, Vol. 21, No. 1, 65-76, doi:10.2507/IJSIMM21-1-588

[12] Chen, N. L.; Zhang, W. M.; Li, Q.; Gao, C. Y.; Liao, B.; Pan, J. S. (2006). Optimization of quench tank structure based on CFD simulation, *Solid State Phenomena*, Vol. 118, 363-368, doi:10.4028/www.scientific.net/SSP.118.363

[13] Chen, N.; Liao, B.; Pan, J.; Li, Q.; Gao, C. (2006). Improvement of the flow rate distribution in quench tank by measurement and computer simulation, *Materials Letters*, Vol. 60, No. 13-14, 1659-1664, doi:10.1016/j.matlet.2005.11.102

[14] Yang, X.-W.; Zhu, J.-C.; He, D.; Lai, Z.-H.; Nong, Z.-S.; Liu, Y. (2013). Optimum design of flow distribution in quenching tank for heat treatment of A357 aluminum alloy large complicated

thin-wall workpieces by CFD simulation and ANN approach, *Transactions of Nonferrous Metals Society of China*, Vol. 23, No. 5, 1442-1451, doi:10.1016/S1003-6326(13)62615-1

[15] Fu, P.; Zhou, P.; Xie, Z.-W.; Wu, H.-Y.; Chen, J. G. (2019). Experimental and CFD investigations on cooling process of end-quench test, *Transactions of Nonferrous Metals Society of China*, Vol. 29, No. 11, 2440-2446, doi:10.1016/S1003-6326(19)65150-2

[16] Qu, Z.; Zhu, X. S.; Xing, R. F.; Fu, Y. D. (2021). Design and fluid-thermal coupling of a strong quenching tank with double vortex flow field, *Heat Treatment of Metals*, Vol. 46, No. 11, 262-269, doi:10.13251/j.issn.0254-6051.2021.11.048

[17] Zhang, J. K.; Zhang, R. M.; Chen, Y. Y.; Song, X. N. (2011). Simulation on temperature field during cooling process on roller-type quenching machine, *Heat Treatment of Metals*, Vol. 36, No. 10, 85-88, doi:10.13251/j.issn.0254-6051.2011.10.026

[18] Zhang, W. L.; Chen, R. Z.; Li, X. J.; Luo, P.; Song, J. S. (2020). Numerical simulation and optimization design of quenching tank for large aluminum ring, *Heat Treatment Technology and Equipment*, Vol. 41, No. 3, 10-15, doi:10.19382/j.cnki.1673-4971.2020.03.002

[19] Wang, K. J.; Yan, S. B.; Lu, Y. M.; Zhuo, T.; Zhang, Y.; Li, X. J. (2022). Numerical simulation and optimal design of quenching tank circulation system of combined well-type unit, *Heat Treatment Technology and Equipment*, Vol. 43, No. 1, 37-40, doi:10.19382/j.cnki.1673-4971.2022.01.009

[20] Cebo-Rudnicka, A.; Malinowski, Z. (2019). Identification of heat flux and heat transfer coefficient during water spray cooling of horizontal copper plate, *International Journal of Thermal Sciences*, Vol. 145, Paper 106038, 24 pages, doi:10.1016/j.ijthermalsci.2019.106038

[21] Li, N.; Yang, C. F.; Pan, T. (2008). Analysis on section effect of heavy plate by finite element method during controlled cooling, *Materials Science Forum*, Vol. 575-578, 1407-1413, doi:10.4028/www.scientific.net/MSF.575-578.1407

[22] Liu, L.; Xie, G. Z.; Wang, Y. H. (2013). Optimizing accelerated cooling processes of thick plates by using numerical simulation, *Materials and Manufacturing Processes*, Vol. 28, No. 1, 56-60, doi:10.1080/10426914.2012.700158

[23] Arora, H.; Singh, R.; Brar, G. S. (2019). Prediction of temperature distribution and displacement of carbon steel plates by FEM, *Materials Today: Proceedings*, Vol. 18, Part 7, 3380-3386, doi:10.1016/j.matpr.2019.07.264

[24] Lee, K. S.; Eom, D. H.; Kim, S. W.; Lee, S. S.; Chun, S. H.; Kim, C. H.; Lee, J. H. (2010). A study on temperature distribution and curved structure for thick plate by single-pass induction heating, *AIP Conference Proceedings*, Vol. 1252, 659-665, doi:10.1063/1.3457618

[25] Dedov, A. V. (2019). A review of modern methods for enhancing nucleate boiling heat transfer, *Thermal Engineering*, Vol. 66, No. 12, 881-915, doi:10.1134/S0040601519120012

[26] Luo, T.; Wang, S. R.; Zhang, C. G.; Liu, X. L. (2017). Parameters deterioration rules of surrounding rock for deep tunnel excavation based on unloading effect, *DYNA*, Vol. 92, No. 6, 648-654, doi:10.6036/8554

[27] Wang, S. R.; Xiao, H. G.; Zou, Z. S.; Cao, C.; Wang, Y. H.; Wang, Z. L. (2019). Mechanical performances of transverse rib bar during pull-out test, *International Journal of Applied Mechanics*, Vol. 11, No. 5, Paper 1950048, 15 pages, doi:10.1142/S1758825119500480